

Fine tuning of optical transition energy of twisted bilayer graphene via interlayer distance modulation

Elena del Corro,^{1,*} Miriam Peña-Alvarez,^{1,2} Kentaro Sato,³ Angel Morales-Garcia,⁴ Milan Bousa,^{1,5} Michal Mračko,⁶ Radek Kolman,⁶ Barbara Pacakova,⁷ Ladislav Kavan,¹ Martin Kalbac,¹ and Otakar Frank^{1,†}

¹*J. Heyrovsky of Institute of Physical Chemistry of the CAS, v.v.i., Dolejskova 2155/3, 182 23 Prague 8, Czech Republic*

²*Departamento de Química Física I, Facultad de Ciencias Químicas, Universidad Complutense de Madrid, 28040, Spain*

³*National Institute of Technology, Sendai College, Sendai 989-3128, Japan*

⁴*Department of Physical and Macromolecular Chemistry, Faculty of Science, Charles University in Prague, Hlavova 2030, Prague 2, 128 43, Czech Republic*

⁵*Department of Inorganic Chemistry, Faculty of Science, Charles University in Prague, Hlavova 2030, Prague 2, 128 43, Czech Republic*

⁶*Institute of Thermomechanics of the CAS, v.v.i., Dolejskova 1402/5, CZ 182 23 Prague 8, Czech Republic*

⁷*Institute of Physics of the CAS, v.v.i., Na Slovance 2, 182 21, Prague 8, Czech Republic*

(Received 22 July 2016; revised manuscript received 14 December 2016; published 23 February 2017)

Twisted bilayer graphene (tBLG) represents a family of unique materials with optoelectronic properties tuned by the rotation angle between the two layers. The presented work shows an additional way of tweaking the electronic structure of tBLG by modifying the interlayer distance, for example by a small uniaxial out-of-plane compression. We have focused on the optical transition energy, which shows a clear dependence on the interlayer distance, both experimentally and theoretically.

DOI: [10.1103/PhysRevB.95.085138](https://doi.org/10.1103/PhysRevB.95.085138)

I. INTRODUCTION

Since the advent of graphene, tuning of its electronic structure has been one of the strongest focal points for many researchers. However, so far the vision of exploiting the unique properties of graphene for the replacement of silicon in electronics has been hampered by the inability to open a sizable band gap in a simple, controlled, and cost-effective manner [1]. For this purpose, bilayer graphene (BLG) holds more promise, for applications such as nanoelectronics, than monolayer graphene, as it offers several routes of profiting from the interactions between the two layers [2–4], e.g., by dual gating [4,5], molecular doping [6], or theoretically by mechanical deformation [7]. Similarly, the appealing concept of a bilayer pseudospin field effect transistor (BiSFET) still exists only at the theoretical level [3,8,9]. The interlayer distance could be one of the important parameters controlling the excitonic gap in BiSFET [10].

Twisted bilayer graphene (tBLG), i.e., a system where the alignment of the two graphene layers deviates from the periodic (AB) Bernal stacking, has recently attracted increased attention. In fact, each tBLG with a particular twist angle represents a unique material in terms of its optoelectronic properties [11]. The relative rotation of the layers leads to the formation of a superlattice, which manifests itself as Moiré patterns in high-resolution transmission electron microscopy [12] or scanning tunneling microscopy [13] studies. Importantly, the interference in superlattices gives rise to van Hove singularities (vHS) in the density of states (DOS), with their energy gap dependent on the twist angle [12–14]. The vHS cause optical coloration of the tBLG [11] and a strong resonance enhancement of the Raman *G* mode when the laser excitation matches the vHS energy [12,15,16].

As mentioned above, the interaction between the two layers depends on the twist angle; however, the influence of the interlayer distance has never been examined. Moreover, the interlayer space in stacked two-dimensional materials provides an additional feature through the so-called van der Waals pressure acting upon molecules or crystals trapped in between the layers [17,18]. However, this phenomenon is still to be fully explained.

In the presented work we have studied tBLG of various origin under direct uniaxial out-of-plane compression in a low stress regime. Simultaneous *in situ* Raman spectroscopy measurement revealed a clear modulation of the *G* band enhancement, indicating changes in the resonance conditions and hence in the energy of the vHS. In order to evaluate the effect of compression, we have performed theoretical calculations of the DOS of tBLG, modulating both the interlayer and the in-plane C-C distance. Our calculations reveal variations of the vHS energy as a dependence of the interlayer distance, as large as 200 meV, while negligible variations are detected when decreasing the *a* lattice parameter.

II. MATERIALS AND METHODS

Experiments. Single layer graphene samples of ¹²C and ¹³C were prepared using the CVD method, described elsewhere [19]. Labeled bilayer graphene was obtained by sequential transfer of individual monolayers from copper foil onto a sapphire disk, using the reported wet transfer method with polymethylmethacrylate [20]. Additionally, as-grown and exfoliated ¹²C BLG samples were studied for comparison. The experimental setup consisted of a gem anvil cell coupled to a Raman spectrometer (LabRAM HR, Horiba Jobin-Yvon). In order to perform direct out-of-plane compression, a modified sapphire cell was used, with one anvil substituted by a sapphire disk containing the sample. In such conditions, the use of a conventional stress marker is inadequate and therefore,

*Corresponding author: edelcorro@quim.ucm.es

†Corresponding author: otakar.frank@jh-inst.cas.cz

stress was estimated from the evolution of the Raman peaks of sapphire [21]. Raman spectra and maps were registered using an Ar⁺/Kr⁺ laser working at 488.0, 514.5, 532.0, and 647.1 nm, keeping the power on the sample below 1 mW. A 50 \times objective produced a laser spot on the sample of $\sim 1 \mu\text{m}$ diameter. Grating with 600 grooves mm^{-1} was used to provide spectral point-to-point (pixel) resolution of $\sim 1.8 \text{ cm}^{-1}$ at 488.0 nm excitation wavelength. At each 0.1 and 0.5 GPa compression step single spectra and Raman maps ($20 \times 20 \mu\text{m}^2$, 1–2 μm sampling steps) were registered, respectively, for selected sample grains fulfilling the resonant conditions at the corresponding laser excitation energy.

Calculations. A commensurate structure of tBLG is characterized by two integers (n, m), which define the rotation angle between the layers. In the calculation, we use primitive vectors $\mathbf{T}_1 = n\mathbf{a}_1 + m\mathbf{a}_2$ and $\mathbf{T}_2 = (n + m)\mathbf{a}_1 - n\mathbf{a}_2$ for (n, m) tBLG [14]. Here $\mathbf{a}_1 = a(\sqrt{3}/2, 1/2)$, $\mathbf{a}_2 = a(\sqrt{3}/2, -1/2)$, and $a = |\mathbf{a}_1| = |\mathbf{a}_2|$ are the primitive vectors and lattice constants for monolayer graphene, respectively. The electronic structure and DOS of tBLG are calculated using the tight-binding method [22,23] with a different interlayer distance and in-plane lattice constant in order to evaluate the effect of compression. The adopted tight-binding parameter is a function of the distance between the carbon atoms [22]. The optical transition energy, corresponding to the enhancement effect of Raman intensity, is determined from the results. Optical transitions between the saddle points of the electronic structure are not allowed [24].

III. RESULTS AND DISCUSSION

The Raman spectrum of labeled BLG has been previously reported [25]. The phonon frequency (ω) scales inversely with the square root of atomic mass and, therefore, the Raman peaks from each layer can be distinguished [26]. Thus, the Raman spectrum of labeled BLG is dominated by four peaks: two G bands (1525 and 1590 cm^{-1}) and two $2D$ bands (2620 and 2710 cm^{-1}), with the lower frequency peaks corresponding to ^{13}C [26]. Analogously, in the case where lattice disorder is present in the sample, two D bands appear at ~ 1303 and 1347 cm^{-1} (2.54 eV excitation energy).

As stated above, tBLG shows vHS in the density of states, with their energy gap dependent on the twist angle. When the excitation wavelength matches the energy difference between these vHS (the optical transition energy), an enhancement of the G band intensity is observed, and the $G/2D$ intensity ratio (amplitudes) increases by a factor of 15, see Fig. 1, or even more depending on the sample. In order to locate tBLG grains in resonance with the excitation energy used, Raman maps of $40 \times 40 \mu\text{m}^2$ were measured with distinguishable regions exhibiting enhanced G band (see Fig. S2 [27]). In Figure 2(a) we show single Raman spectra acquired at the center of a tBLG grain, fulfilling the resonant conditions at 2.54 eV excitation energy, i.e., $\sim 13^\circ$ rotation angle [12]. We sequentially increase the out-of-plane compression up to approximately 1.6 GPa. The use of isotopically labeled tBLG allows us to bring to light any potential disharmony in the evolution of the two layers during the high stress experiment. However, Fig. 2 shows that both layers in the examined tBLG (and in all other experimental runs mentioned further) manifest the same behavior under compression.

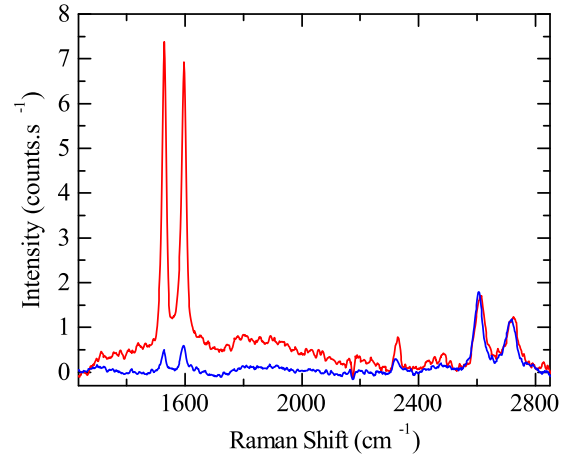


FIG. 1. Raman spectra of the $^{13}\text{C}/^{12}\text{C}$ tBLG at ambient conditions, with and without G band enhancement at the laser excitation wavelength of 488.0 nm. The spectra are normalized to the $2D$ band amplitude.

As shown for graphite [28] and other layered materials [29], out-of-plane compression decreases, preferentially, the distance between layers. In other words, the out-of-plane compressibility is much higher than the in-plane compressibility, owing to weak interlayer forces. At the initial stages of compression (up to 0.4 GPa), we observe an increase in the G band enhancement by a factor of ~ 1.5 [the increase in the G band enhancement can reach a factor of 4, depending on the sample, see Fig. 3(a)], followed by a decrease to the original value at about 0.7 GPa. Such a variation indicates that the decrease in the interlayer distance modifies the resonance conditions, i.e., the electronic properties of the system. During the later stages of compression, above 1 GPa, the enhancement continues decreasing due to other factors affecting the compression experiment, such as the sample disorder, as reported before [30] and discussed in the Supplemental Material, Fig. S3 [27].

The G band enhancement within the 0.5 GPa range warrants further investigation. In Fig. 2(b) we present the stress performance during consecutive compression cycles of a tBLG grain. We have observed that the behavior described above is reversible in the low stress range. Such reversibility confirms the assumption that the change in the interlayer distance is the main factor of the modulation of the tBLG electronic properties. While the charge doping has been shown to modify the electron resonance in tBLG [31], a possible change in the doping state induced by an irreversible purging of impurities (remnant from the transfer process) from the interlayer space, can be ruled out based on the reversible behavior shown in Fig. 2(b). A change of rotation angle with shear stress can also be excluded as an explanation of the G band enhancement in view of Fig. 2(b). Moreover, additional observations based on the finite elements (FE) method, compiled in the Supplemental Material [27], demonstrate only insignificant shear stresses, at least three orders of magnitude smaller than the out-of-plane compressive forces, hence no appreciable relative movement of the layers is expected [32].

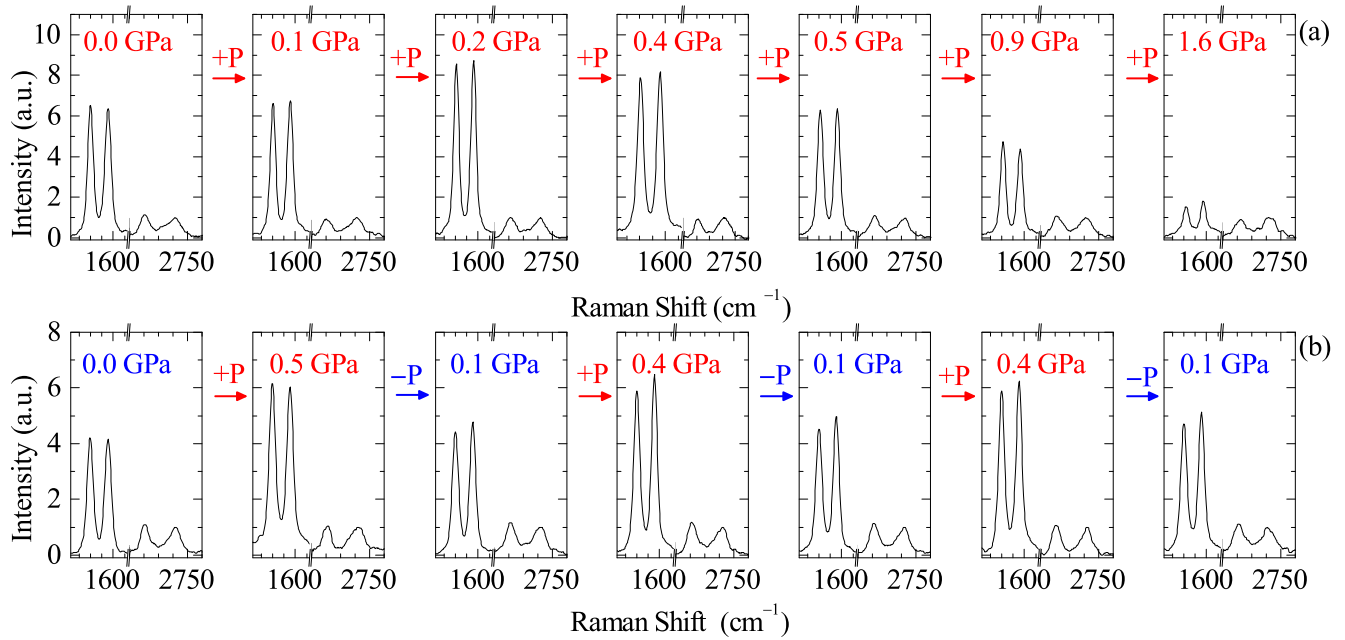


FIG. 2. Evolution of Raman spectra of $^{13}\text{C}/^{12}\text{C}$ tBLG (a) with compression up to 1.6 GPa, and (b) with stress cycling of approximately ± 0.4 GPa. The laser excitation wavelength is 488.0 nm. The spectra are normalized to the 2D band amplitude in each plot.

In order to prove the universality of our findings, additional experiments were performed by employing several excitation energies and analyzing different tBLG samples. In Fig. 3(a) we present the evolution of the $G/2D$ amplitude ratio with increasing stress for labeled tBLG with different twist angles; each of them excited with the corresponding resonant laser energy in order to observe G band enhancement (for the same plot, but with ratio of $G/2D$ integrated areas, see Fig. S11 in the Supplemental Material [27]). We observed that the variation of the resonant conditions is qualitatively the same regardless of rotation angle and excitation energy. Grains with different twist angles exhibit different magnitudes of energy band-gap

modulation, as evidenced by the varying enhancement factor and position of the enhancement maximum for individual excitation wavelengths in Fig. 3(a), and as demonstrated by our theoretical calculations in the last section.

In Fig. 3(b) we compare the compression behavior of as-grown ^{12}C tBLG with that prepared by a sequential transfer of two monolayers. The latter shows a compression behavior analogous to the labeled tBLG. Note that before compression, the sample consists of two layers of graphene sequentially transferred, in which remnant polymers or other impurities from the transfer process may hinder a closer contact between them (see AFM analysis in the Supplemental Material, Fig. S10 [27]). However, in the as-grown tBLG samples, the graphene layers are in closer contact in their original state, and therefore the increase in G band enhancement is almost absent. Note that the maximum stress-induced enhancement in the sequentially transferred tBLG is the same as the initial enhancement in the as-grown tBLG.

To further prove the effect of interlayer distance on the resonant conditions and therefore on the electronic properties of tBLG, we performed a single compression cycle up to 0.6 GPa on a tBLG grain with a G band enhancement manifested for both the 488.0 and 514.5 nm excitation wavelengths. Note that the G band enhancement is not the maximum possible for either of the excitation energies, which indicates that the rotation angle of the measured grain is between 13.0 and 12.3 deg (see Fig. 4). When increasing the stress, thereby reducing the interlayer distance, resonant conditions are changed in such a way that the same grain more closely fulfills resonance conditions for 488.0 nm, while simultaneously, enhancement is almost lost for the 514.5 nm line. This result indicates that the optical transition energy for the analyzed tBLG grain has increased upon compression, abruptly moving closer to 2.54 eV (488.0 nm) rather than to 2.41 eV (514.5 nm), followed by a stabilization of the energy after applying a stress of ~ 0.5 GPa.

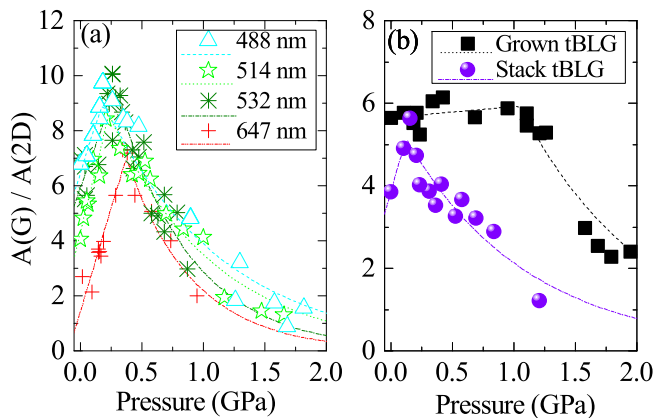


FIG. 3. Evolution of the $G/2D$ amplitude ratio with increasing stress: (a) Labeled tBLG with rotation angles of 13.0°, 12.3°, 11.9°, and 9.8° excited with 488.0, 514.5, 532.0, and 647.1 nm laser wavelengths, respectively, to achieve G band enhancement in each sample [12]. (b) ^{12}C CVD BLG (squares) and $^{12}\text{C}/^{12}\text{C}$ stack BLG (circles); both measured in a region resonant with 488.0 nm excitation wavelength. Dotted lines are guides for the eye.

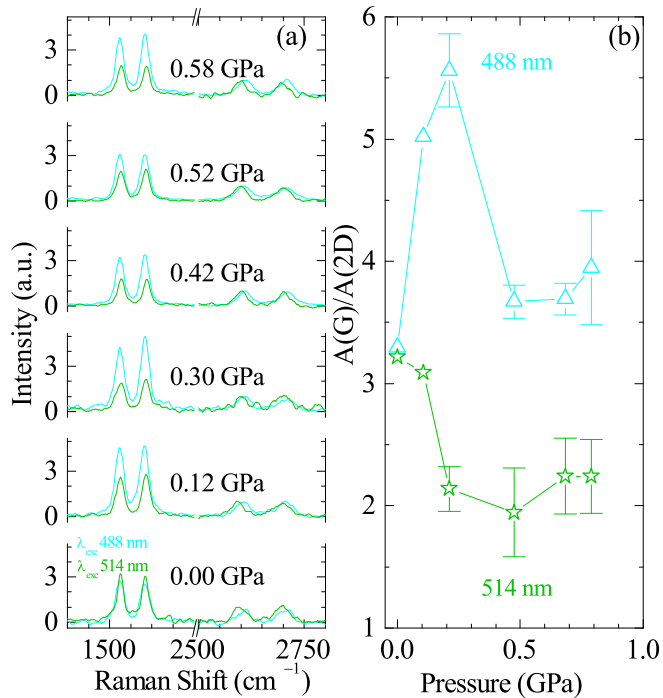


FIG. 4. Evolution of Raman spectra of $^{13}\text{C}/^{12}\text{C}$ tBLG with compression up to 0.6 GPa. (a) The same tBLG grain is measured with 488.0 (blue spectra) nm and 514.5 nm excitation wavelengths (green spectra). Each spectrum is normalized to the 2D band amplitude. (b) $G/2D$ amplitude ratios from (a) as a function of increasing stress.

Finally, modulation of the electronic structure of tBLG in the low stress regime, demonstrated by the G band enhancement, is examined with the aid of calculations based on the tight-binding method. As an example, we present the DOS of the (3,2) tBLG structure in Fig. 5(a) (corresponding to a $\sim 13^\circ$ rotation angle, in resonance with 488.0 nm excitation wavelength [14]) at selected interlayer distances (d) ranging from 0.50 to 0.25 nm. We scan a wide d interval in order to account for all possible experimental variables: the decrease of d by means of stress and the increase of d in pristine samples due to their preparation method [27]. We observed that both the DOS and the vHS energy are modified by d . Specifically, in Fig. 5(b) we see that upon decreasing the interlayer distance to ~ 0.45 nm, the optical transition energy quickly reaches a maximum, and then starts to decrease at a slower pace as layers continue to move closer to each other. This is in perfect agreement with the experimental results presented in Fig. 4, where the initially similar resonance (with 2.41 and 2.54 eV laser excitations) is immediately moved towards 2.54 eV and then steadied. Along the whole analyzed range of interlayer distances, the optical transition energy shows variations as large as 200 meV, for the given twist angle. This variation of optical transition energy with d alters the resonance conditions, thereby explaining the experimental observations where the G band enhancement changes with stress at a particular excitation energy. The theoretical behavior of (1,5) tBLG, which is slightly further from the resonance with a 488.0 nm laser (twist angle of $\sim 15^\circ$), has also been checked; the optical transition energy follows a similar trend as in (3,2) tBLG, albeit with a smaller energy difference, up to 80 meV.

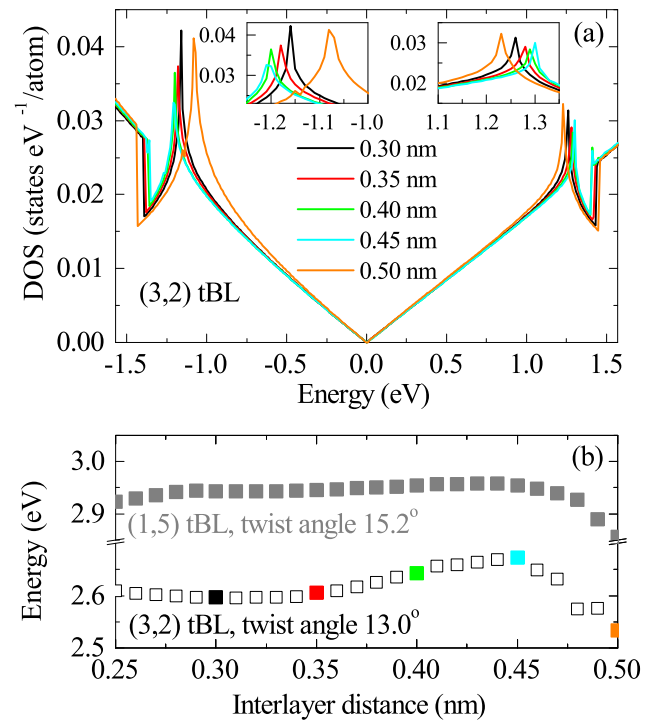


FIG. 5. (a) Density of states of (3,2) tBLG at different interlayer distances. (b) Optical transition energy as a function of the interlayer distance for (3,2) and (1,5) tBLG, labeled with squares and circles, respectively. Highlighted points in the (3,2) tBLG curve in (b) correspond to the curves in (a) with the same color.

As noted above, despite being lower, the tBLG out-of-plane compression demonstrates clear in-plane compressibility [33], proved by the blueshift of the Raman spectrum [27]. The influence of the in-plane compression on the electronic properties of tBLG is presented in Fig. 6. DOS was calculated for the same (3,2) tBLG structure at a fixed interlayer distance (0.35 nm) with decreasing a lattice parameter values, from the equilibrium (0.2460 nm) down to 0.24565 nm (corresponding to an in-plane compression of > 1.5 GPa, obtained from the

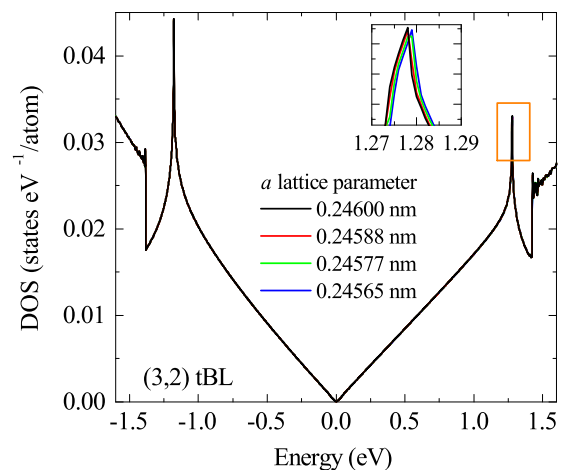


FIG. 6. The density of states of the (3,2) tBLG, with 0.35 nm interlayer distance, as a function of the a lattice parameter.

equation of state of graphite [34]). Within this a range, only a negligible increase of the vHS energy, ~ 1 meV, is observed. Moreover, when decreasing the a parameter more drastically to 0.2435 nm (estimated stress of ~ 10 GPa), the increase in vHS energy obtained theoretically is lower than 10 meV, which is 20 times smaller than the changed observed with the interlayer distance modulation. Thus, according to our calculations, in-plane stress can be discarded as the origin of the modulation of the resonance conditions in tBLG.

IV. CONCLUSIONS

In summary, we have shown the dependence of the energy of van Hove singularities with interlayer distance in tBLG. Various samples of tBLG were subjected to out-of-plane compression and their behavior was monitored *in situ* by Raman spectroscopy using different laser excitation energies. The experiment showed a change in the Raman G band enhancement reflecting the modified resonance conditions caused by the altered vHS energy. The results were corroborated by tight-binding calculations, which revealed an initial

increase in the optical transition energy upon decreasing the interlayer distance to ~ 0.45 nm, where the maximum energy was reached, followed by a gradual decrease with further narrowing of the interlayer gap. The calculations also showed that the in-plane compression of graphene layers was not responsible for the changes in the optical transition energy. The sensitivity of tBLG to interlayer distance can prove valuable in optoelectronic applications, and based on our observations, it also explains the differences in the magnitude of the G band enhancement observed at particular laser excitations for differently prepared samples.

ACKNOWLEDGMENTS

This work was funded by the Czech Science Foundation (GACR 14-15357S), MSM ERC-CZ project (LL 1301), and European Union H2020 Program (Grant No. 696656—GrapheneCore1) and JSPS KAKENHI (Grant No. JP15K17437). K.S. acknowledges support from MEXT (Grant No. 23710118). M.M. and R.K. acknowledge the Czech Science Foundation (GACR 16-03823S) within the institutional support RVO 61388998.

-
- [1] F. Schwierz, *Nat. Nanotechnol.* **5**, 487 (2010).
 [2] M. Edward and K. Mikito, *Rep. Prog. Phys.* **76**, 056503 (2013).
 [3] L. F. Register, X. Mou, D. Reddy, W. Jung, I. Sodemann, D. Pesin, A. Hassibi, A. H. MacDonald, and S. K. Banerjee, *ECS Trans.* **45**, 3 (2012).
 [4] T. Ohta, A. Bostwick, T. Seyller, K. Horn, and E. Rotenberg, *Science* **313**, 951 (2006).
 [5] E. V. Castro, K. S. Novoselov, S. V. Morozov, N. M. R. Peres, J. M. B. L. dos Santos, J. Nilsson, F. Guinea, A. K. Geim, and A. H. Castro Neto, *Phys. Rev. Lett.* **99**, 216802 (2007).
 [6] W. Zhang *et al.*, *Acs Nano* **5**, 7517 (2011).
 [7] C. Galiotis, O. Frank, E. N. Koukaras, and D. Sfyris, *Annu. Rev. Chem. Biomol. Eng.* **6**, 121 (2015).
 [8] S. K. Banerjee, L. F. Register, E. Tutuc, D. Reddy, and A. H. MacDonald, *IEEE Electron Device Lett.* **30**, 158 (2009).
 [9] H. Min, R. Bistritzer, J.-J. Su, and A. H. MacDonald, *Phys. Rev. B* **78**, 121401 (2008).
 [10] I. Sodemann, D. A. Pesin, and A. H. MacDonald, *Phys. Rev. B* **85**, 195136 (2012).
 [11] J. Campos-Delgado, G. Algara-Siller, C. N. Santos, U. Kaiser, and J. P. Raskin, *Small* **9**, 3247 (2013).
 [12] K. Kim, S. Coh, L. Z. Tan, W. Regan, J. M. Yuk, E. Chatterjee, M. F. Crommie, M. L. Cohen, S. G. Louie, and A. Zettl, *Phys. Rev. Lett.* **108**, 246103 (2012).
 [13] G. Li, A. Luican, J. M. B. Lopes dos Santos, A. H. Castro Neto, A. Reina, J. Kong, and E. Y. Andrei, *Nat. Phys.* **6**, 109 (2010).
 [14] H. B. Ribeiro, K. Sato, G. S. N. Eliel, E. A. T. de Souza, C.-C. Lu, P.-W. Chiu, R. Saito, and M. A. Pimenta, *Carbon* **90**, 138 (2015).
 [15] A. Jorio and L. G. Cançado, *Solid State Commun.* **175-176**, 3 (2013).
 [16] M. Kalbac, O. Frank, J. Kong, J. Sanchez-Yamagishi, K. Watanabe, T. Taniguchi, P. Jarillo-Herrero, and M. S. Dresselhaus, *J. Phys. Chem. Lett.* **3**, 796 (2012).
 [17] E. Khestanova, F. Guinea, L. Fumagalli, A. K. Geim, and I. V. Grigorieva, *Nat. Commun.* **7**, 12587 (2016).
 [18] K. S. Vasu *et al.*, *Nat. Commun.* **7**, 12168 (2016).
 [19] M. Kalbac, H. Farhat, J. Kong, P. Janda, L. Kavan, and M. S. Dresselhaus, *Nano Lett.* **11**, 1957 (2011).
 [20] X. Li, Y. Zhu, W. Cai, M. Borysiak, B. Han, D. Chen, R. D. Piner, L. Colombo, and R. S. Ruoff, *Nano Lett.* **9**, 4359 (2009).
 [21] E. del Corro, M. Taravillo, J. González, and V. G. Baonza, *Carbon* **49**, 973 (2011).
 [22] G. Trambly de Laissardière, D. Mayou, and L. Magaud, *Nano Lett.* **10**, 804 (2010).
 [23] A. Grüneis, C. Attacalite, L. Wirtz, H. Shiozawa, R. Saito, T. Pichler, and A. Rubio, *Phys. Rev. B* **78**, 205425 (2008).
 [24] P. Moon and M. Koshino, *Phys. Rev. B* **87**, 205404 (2013).
 [25] P. T. Araujo, O. Frank, D. L. Mafra, W. Fang, J. Kong, M. S. Dresselhaus, and M. Kalbac, *Sci. Rep.* **3**, 2061 (2013).
 [26] O. Frank, L. Kavan, and M. Kalbac, *Nanoscale* **6**, 6363 (2014).
 [27] See Supplemental Material at <http://link.aps.org/supplemental/10.1103/PhysRevB.95.085138> for additional Raman spectroscopy data, characterization and simulation of the anvil experiment, atomic force microscopy images, and additional tight-binding calculations of the electronic structure of tBLG.
 [28] D. Abbasi-Pérez, J. M. Menéndez, J. M. Recio, A. Otero-de-la-Roza, E. del Corro, M. Taravillo, V. G. Baonza, and M. Marqués, *Phys. Rev. B* **90**, 054105 (2014).
 [29] M. Peña-Álvarez, E. del Corro, Á. Morales-García, L. Kavan, M. Kalbac, and O. Frank, *Nano Lett.* **15**, 3139 (2015).
 [30] S. W. Schmucker, C. D. Cress, J. C. Culbertson, J. W. Beeman, O. D. Dubon, and J. T. Robinson, *Carbon* **93**, 250 (2015).
 [31] C.-H. Yeh, Y.-C. Lin, Y.-C. Chen, C.-C. Lu, Z. Liu, K. Suenaga, and P.-W. Chiu, *ACS Nano* **8**, 6962 (2014).
 [32] E. del Corro, M. Peña-Álvarez, M. Mračko, R. Kolman, M. Kalbáč, L. Kavan, and O. Frank, *Phys. Status Solidi B* **253**, 2336 (2016).
 [33] E. del Corro, M. Taravillo, and V. G. Baonza, *Phys. Rev. B* **85**, 033407 (2012).
 [34] M. Hanfland, H. Beister, and K. Syassen, *Phys. Rev. B* **39**, 12598 (1989).